Study of multifrequency sensitivity to soil moisture variations in the lower Bermejo basin

Cristina Vittucci[1]*, Leila Guerriero[1], Paolo Ferrazzoli[1], Rachid Rahmoune[1], Veronica Barraza[2] and Francisco Grings[2]

[1]Department of Civil Engineering and Computer Science Engineering – DICII, Tor Vergata University, Via del Politecnico 1, 00133 - Rome, Italy
[2]Instituto de Astronomía y Física del Espacio - IAFE, Ciudad Universitaria, Casilla de Correo 67 - Suc. 28, 1428 – Buenos Aires, Argentina
*Corresponding author, e-mail address: vittucci@disp.uniroma2.it

Abstract

In this paper, a sensitivity analysis to soil moisture variations as a rain effect has been performed at several microwave bands over the lower Bermejo basin, a subtropical area of Argentina mostly spread by moderately dense forests. Parameters such as emissivity and Polarization Index have been considered to carry out the study. In particular, the performance of L-band SMOS measurements has been compared with C and X band AMSR-E one, highlighting the better achievement of the lower frequencies due to the weaker interaction with the vegetation structures. This work intends to give a contribution in the subject of soil moisture sensitivity, which is a preliminary step in the development of retrieval algorithms.
Keywords: Microwave radiometry, AMSR-E, SMOS, soil moisture, forest.

Introduction

Soil Moisture Content (SMC) is an important boundary condition in land surface processes related to evaporation rate, surface run-off, infiltration and percolation to the water table. Furthermore, SMC is requested as input to forecast models and for agricultural purposes. It is a key surface parameter and, in order to fully understand its role, there is a need of SMC measurements. Remote sensing offers a unique opportunity to collect spatial datasets over large areas, though it is possible to monitor only the top few centimeters of the soil, i.e., the most exposed to the atmosphere where SMC varies in response to rainfall. Active microwave remote sensing provides a source of information, but roughness and vegetation act as disturbances which limit the soil moisture retrieval accuracy. Passive microwave radiometry, besides being independent of weather and day-light, offers a high temporal resolution, which is one of the main requirements for an appropriate monitoring. Despite the coarse spatial resolution, several studies proved the potential for measuring soil moisture with the use of microwave radiometers such as the Advanced Microwave

Scanning Radiometer for EOS (AMSR-E) that works in a wide range of frequencies, from Ka, to X and C bands. [Njoku et al., 2003; Paloscia et al., 2006].

Soil and vegetation conditions affect the microwave measurements through complex interactions, and the influence of vegetation depends, in particular, on the overall biomass [Jackson and Schmugge, 1991]. Several models have been proposed to estimate the microwave emission of soil and the effects of vegetation, and investigations of radiometric properties of forests can be found in experimental and theoretical studies done in the last decades [Ferrazzoli and Guerriero, 1996; Pampaloni, 2004]. It is well known that the presence of vegetation reduces the sensitivity of the microwave measurements to the soil moisture but, since vegetation attenuation increases as wavelength decreases, longer wavelengths are preferred for soil moisture studies [Jackson and Schmugge, 1991]. In view of the availability of the ESA Soil Moisture and Ocean Salinity (SMOS) radiometer and dissemination of its data, several works began to prove the effectiveness of L-band radiometry [Ferrazzoli et al., 2002; Della Vecchia et al., 2007; Kerr et al., 2012], which has been shown to have a good sensitivity to soil moisture variations. However, ground based experiments at L-band did not give a definite indication about soil moisture sensitivity in forested areas: some works reported low effects [Grant et al., 2007], while others showed moderate sensitivity [Santi et al., 2009]. On the other hand, AMSR-E signatures are usually disregarded when dealing with soil moisture below forest covers, since the high canopy attenuation at the employed high frequencies can hide soil contributions, but moderately dense dry forests are worth to be specifically investigated.

To our knowledge, the direct comparison between data acquired over the same area from satellite platforms, in a large frequency range, has not yet been performed. This work intends to give a contribution in the subject of soil moisture sensitivity which is a preliminary step in the development of retrieval algorithms. Indeed, climatic and land cover conditions affect the radiometric response, so that investigations of extended data sets of diverse origins are needed to assess the full potentiality of microwave radiometric measurements.

The aim of this work is to investigate and compare the sensitivities to SMC at C, X and L bands, using the emissivity (e) and the Polarization Index (PI) measured by AMSR-E and SMOS along a two year period. The analysis has been carried out over the Bermejo lower basin, a continental region in Argentina, characterized by moderate forest coverage and subtropical climate. The SMC data, provided by the European Center for Medium-range Weather Forecasts (ECMWF), have been considered, and their temporal trend has been checked against ground rainfall data. The latter were provided by the Comision Regional del Rio Bermejo (http://www.corebe.org.ar) and were collected by some meteorological stations located in the study area.

Site

The region of interest lies between the Chaco and Formosa provinces in the southern part of the Bermejo basin. The basin extends over some 123,000 km², from Andean region to Paraguay River. Crossing different topographic regions, the basin includes an array of rain forest, humid valleys, and mountain desert in the upper part and dry, humid and gallery forest in the lower part.

This area is affected by flood events caused by local precipitations, during the period from October to December, and by the frequent precipitations in the basin, during the period from November to March (85% of total amount of rain). The dry season coincides with autumn - winter in the months of June, July and August when very little or almost no

precipitation occurs. Annual rainfall is characterized by a decrease from east (1400 mm) to west (300 mm), with highest values in the Paraguay River. In that area the river course is characterized by a flat topography with a low slope of 0.2 m/km, appearing in hydrographic network deviations caused by morphological and geological factors. Average temperatures in this period range between 8 and 15° C, with extreme minimum between 0 and -13 ° C, while in summer temperature varies between 16 and 28° C, with extreme maximum between 35 and 45° C, depending on the area. This region presents subtropical characteristics, due to variations that reflect continental climate based on a real winter season. The study area is contained between -27 and -25 S Latitude and -58 and -60 W Longitude. The presence of numerous streams and wetlands produces a regulatory effect, since the rainwater is stored and, after exceeding a certain level, it is drained by the channels.

Dataset

Two datasets composed by AQUA AMSR-E and SMOS MIRAS data have been collected for the time frame 2010-2011. The analysis has been carried out considering the electromagnetic features at C, X and L band. The Ka band has been also taken into account in order to estimate the emissivity at 6.9 and 10.7 GHz, as will be shown in the following Section. Simultaneous rain measurements acquired by meteorological stations located on the basin have been also included in the study.

The Advanced Microwave Scanning Radiometer for EOS (AMSR-E), aboard NASA's AQUA satellite, provides measurements of horizontally and vertically polarized brightness temperature (T_B) at 6.9 GHz, 10.7 GHz, 18.7 GHz, 23.8 GHz, 36.5 GHz, and 89.0 GHz. The mean spatial resolution at the frequencies considered in this work are equal to 56 km at C-band, 38 km at X-band and 12 km at Ka-band with an incidence angle of 54.8° on the Earth's surface. AMSR-E operates in a Sun-synchronous orbit at 98.2° inclination with ascending equator crossings at 13:30 LT. The imaged swath width is 1445 km, providing full global coverage within 3 days [Kawanishi et al., 2003]. Data from AMSR-E level 2 (L2) have been collected, at both polarizations and in descending orbits, yielding measurements from January 1st 2010 to October 4th 2011, when AMSR-E activity was interrupted.

The Soil Moisture and Ocean Salinity (SMOS) ESA satellite provides continuous multi angular measurements of brightness temperature at a frequency of 1.4 GHz. This frequency provides the best sensitivity to variations of moisture in the soil and changes in the salinity of the ocean, coupled with minimal disturbance from weather, atmosphere and vegetation cover [Kerr et al., 2012]. In order to achieve the best spatial resolution, the Microwave Imaging Radiometer with Aperture Synthesis (MIRAS) instrument was developed: it simulates a synthetic antenna composed by 69 small antennas, distributed over three arms and central hub of the instrument. MIRAS is a 2D interferometer yielding a range of incidence angles from 0° to 55° at both V and H polarizations, and a 1,000 km swath width. Its multi-incidence angle capability is expected to assist in determining ancillary data requirements such as vegetation attenuation [Kerr et al., 2001]. Daily L1C observations from ascending and descending orbits have been acquired for the same interval of time of AMSR-E. The L1C T_B data have been extracted averaging measurements with an observational angle within 37.5° and 47.5°. Indeed, the best quality data fall in this range, while data at larger angles are quite few. Finally, samples collected at the swath borders have been deleted, since only averages performed over more than 100 samples have been retained.

For the aims of this study, also L2 Data Analysis Product (DAP), containing ECMWF auxiliary products, like SMC and the surface temperature (Ts), have been considered. Finally, the daily rainfall recorded during 2010 and 2011 at 4 meteorological stations (Gral Vedia, Puerto Bermejo, El Colorado, Laguna Limpia) are included in the study. These measurements account for the soil moisture conditions of the El Colorado site (-26.30 S; -58.30 W), which is considered in this study (Fig. 1).
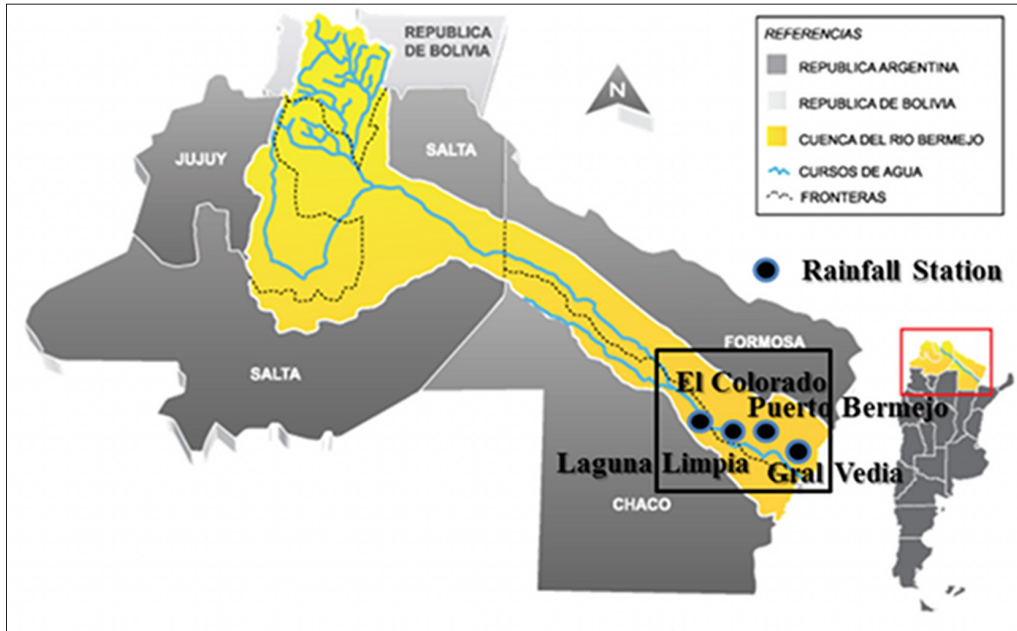

Figure 1 - Bermejo basin Map. The black frame shows the study area. The rainfall stations considered in the analysis are marked by circles.

Methodology

Daily L2 AMSR-E and L1C SMOS products have been considered to extract brightness temperatures at C, X, Ka and L bands, averaging the values in a square window of 0.5 degree in latitude and longitude with the center on El Colorado station location. In order to eliminate the dependence on surface temperature, the emissivity has been computed. Since the two radiometric measurements are performed at different local times, two different values of surface temperatures have been used, which guarantee the closest correspondence to the satellite acquisitions. The T_B's at C and X bands have been used to estimate the corresponding surface emissivities e applying the following formula:

$$e_{pf} = \frac{T_{Bpf}}{T_s} \quad [1]$$

where T_{Bpf} is the brightness temperature at the selected frequency f and polarization p (V or H), while T_S is the surface temperature computed as

$$T_S = 0.94\, T_{BvK_a} + 30.8 \quad [2]$$

where T_{BvKa} is the K_a brightness temperature at Vertical polarization [Parinussa et al., 2012]. The emissivity at L band has been computed applying eq. 1, considering the T_S extracted from DAP auxiliary products and evaluated applying the procedure described in Kerr et al. [2012].

In order to compare the surface temperatures estimated through the two methods, Figure 2 reports the values calculated for those days when both AMSR and SMOS data are acquired. The colours highlight the difference between surface temperature evaluated for the SMOS night-time pass (in red) and those evaluated for SMOS day-time pass (in blue). Both values are displayed versus the temperature derived on the same day by AMSR at descending pass, which crosses the equator at 1:30 AM. As expected the DAP temperatures of the day-time SMOS passes are higher than those of the night-time passes. Furthermore, the data evaluated through the two methods are quite well correlated and it is possible to observe that data depicted in red lay along the plot diagonal, showing that the two methods estimate very similar temperatures when the satellite times of acquisition are the closest, i.e., during the first 6 hours of the day.

In this analysis the Polarization Index (PI) has also been considered. It is defined as

$$PI = \frac{T_{Bv} - T_{Bh}}{0.5\left(T_{Bv} + T_{Bh}\right)} \quad [3]$$

where T_{Bv} and T_{Bh} are the brightness temperature values collected at vertical and horizontal polarization, respectively. This index has been evaluated at C, X, and L bands. In the following section the daily values of e and PI have been plotted together with the ECMWF SMC and rainfall trends in order to verify the soil moisture sensitivity at different wavelengths. Moreover the correlation between the radiometric features and the SMC has been computed at the considered frequencies. Finally, emissivity maps of the study area have been compared to soil moisture maps in order to investigate the spatial variability of the microwave measurements.

Results

It is well known that the emissivity of a bare soil is higher at vertical (V) polarization than at horizontal (H) polarization and, in principle, an increase of the soil moisture content produces a decrease of emissivity at both polarizations, and at all microwave frequencies. This effect is more significant at H polarization and at the lower frequencies [Ulaby et al., 1986]. Change of vegetation coverage, like growth and senescence, influences the difference between vertically polarized and horizontally polarized emission, i.e., the Polarization Index [Paloscia and Pampaloni, 1988]. Other studies pointed out as the same polarization index is also sensitive to soil moisture, at least at frequencies lower than 10 GHz [Ferrazzoli et al., 1992], and it is useful to detect events influencing SMC, like rainfall and flooding [Njoku et al., 2003].
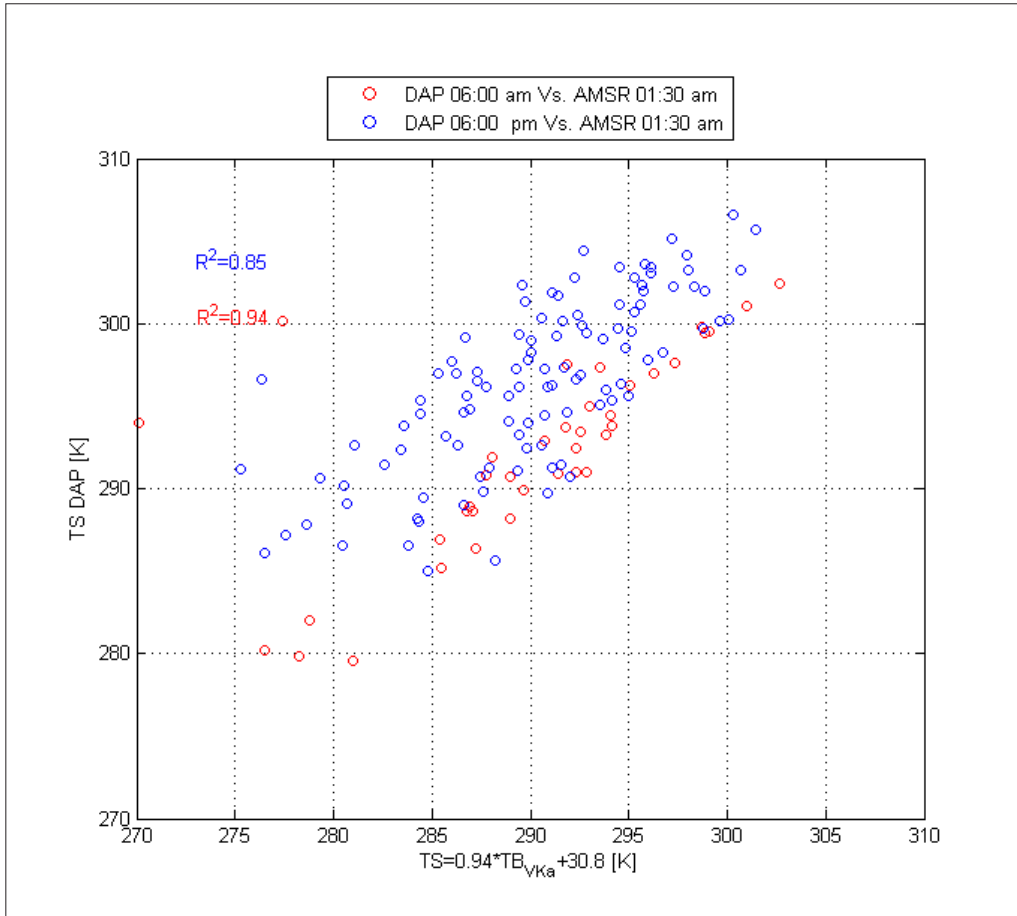
Figure 2 - Scatterplot reporting the surface temperature values calculated for those days when both AMSR and SMOS data are acquired. The surface temperature evaluated for the SMOS night-time pass (6:00 am) versus the temperature derived on the same day by AMSR at descending pass (1.30 am) are plotted in red. The surface temperature evaluated for the SMOS day-time pass (6:00 pm) versus the temperature derived on the same day by AMSR at descending pass (1:30 am) are plotted in blue.

In Figure 3 the temporal trends of PI at three frequencies, ECMWF soil moisture and rainfall vs. the Day of Year (DoY) are shown. In general, a rain event corresponds to an increase of SMC, while dry periods correspond to lower SMC values. The first and last fifty days of each year (December to February) represent the most rainy period. During this season, the change in SMC may appear after some days from the rain event because of soil saturation. From June to August (DoY = 150-250), rainfalls of average magnitude can produce sudden increase of SMC that, on the other hand, show visible decreasing trend during dry periods. The range of SMC variation (between 0.25 and 0.5 m³/m³) is quite significant, although very dry conditions are never met because of the presence of several rivers and wetlands. Literature reports that ECMWF product overestimates soil moisture with a bias of about 0.08 m³/m³, but it reproduces the real dynamics [Al Bitar et al., 2012]. For this reasons,

ECMWF SMC can be considered a valuable tool for a sensitivity study, such as the present one, but cannot be regarded as a ground truth SMC value.
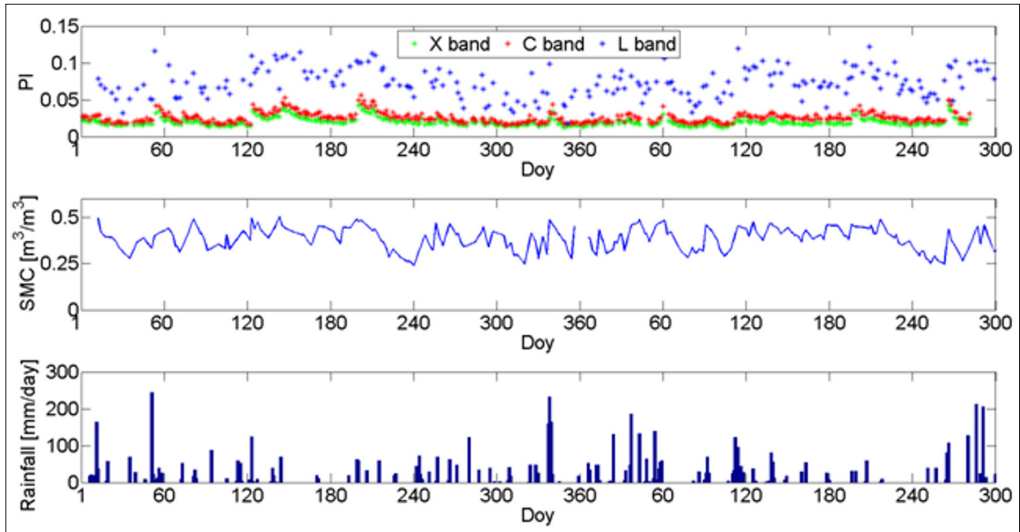

Figure 3 - Temporal trends on El-Colorado site. From top to bottom: Polarization Index at X, C and L band. Soil Moisture by ECMWF [m3/m3]. Rainfall [mm/day].

As it was mentioned in the Introduction, the emission due to biomass may hide the emission of soil. However considering small temporal intervals (from few days to few weeks), PI variations can be related mostly to SMC, especially over forests where the emission due to vegetation can be considered stable. Indeed, forests change very slowly their biomass, so that variations of the vegetation emission contribution are slower than variations due to rainfall or flooding, except when the spaceborne observation takes place just during the rainfall or soon after the rainfalls when interception or change in canopy moisture may occur. In any case, these phenomena produce an unpolarized emission which reduces the difference between vertical and horizontal polarization. These considerations have been applied to the emissivity measured over El-Colorado site, which is mainly covered by open forest dominated by *Schinopsis balansae*. Figure 3 shows that an increase of PI is observed after the main rainfalls (see the upper plot), so that emissivity variations can be related mainly to soil effects. It is then possible to say that, in this case study, variations of remotely sensed parameters are associated to rain events and consequent increases of soil moisture instead of vegetation effects.

In Figure 4 and 5, two enlargements of the previous plots are reported, separating AMSR-E and SMOS data for two periods of about thirty days. Rainfall is also included in the figures. During the rainy period (DoY = 40-70 of 2010) the increase of PI at C and X band is apparent after the stronger rain event, while at L-band a high PI value is maintained for a longer period. During the dry period (DoY = 185-215 of 2011) even a lower amount of rain produces an increase of PI at C and X band. Indeed, this season in the Chaco region corresponds to the austral winter, when trees shed leaves and rainless periods last longer allowing

soil drying. In such situations the occurrence of rainfall of moderate magnitude can produce increases of PI comparable to the one caused by strong rainfall occurring in the wet season.
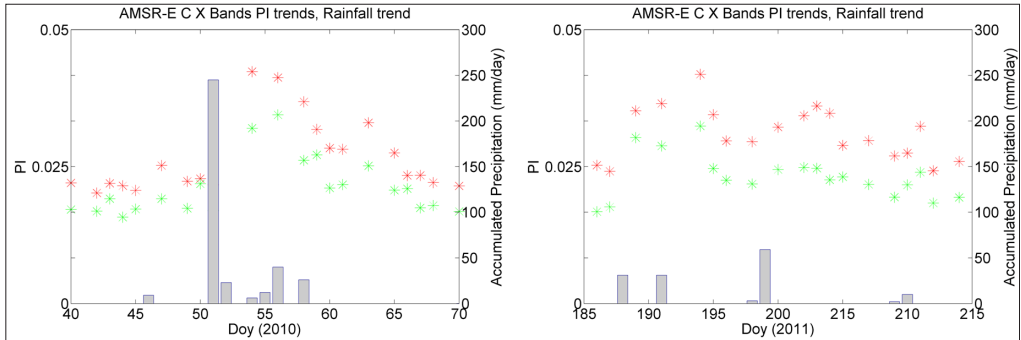

Figure 4 - PI windows at X and C bands on the left in wet period (40-70 DoY 2010); on the right in dry period (185-215 DoY 2011)
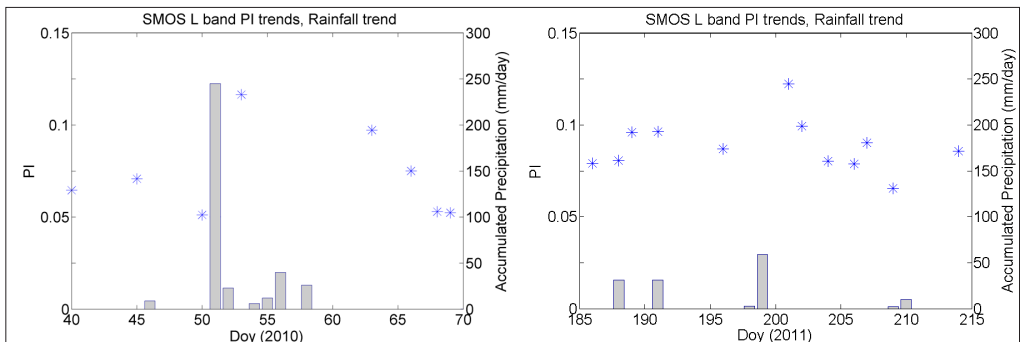

Figure 5 - PI windows at L band on the left in wet period (40-70 DoY 2010); on the right in dry period (185-215 DoY 2011).

From the PI plots, together with the larger data dispersion, the higher dynamics of the L band can be remarked, in comparison to C and X band, due to the deeper penetration capability of the longer wavelength. We also note that at L-band, PI shows a higher sensitivity to SM variations despite of the smaller SMOS observation angle.

In order to better appreciate the sensitivity of microwave emission to SMC, some scatterplots are presented in Figures 6. A general agreement can be noted between the decreasing trend of emissivity and the soil moisture increase at all bands, as well as a confirmation of the higher sensitivity at the lower frequencies in forested areas.

In Figures 6-a,b,c the emissivity at H and V polarizations collected in the timeframe 2010-2011 are plotted vs. ECMWF SMC values. As already mentioned, theoretical and experimental studies indicate that in forests with moderate biomass, the contribution of soil emission is still appreciable at L and C bands [Della Vecchia et al., 2010; Rahmoune et al., 2010]. In order to highlight the soil contribution to the emissivity, the latter has been plotted

separating Spring-Summer and Autumn-Winter data. During the austral Autumn-Winter period of both 2010 and 2011, emissivity presents a more relevant sensitivity to SMC than during Spring-Summer season. This behaviour, mainly due to the absence of leaves, and hence to a lower crown attenuation [Della Vecchia et al., 2010], is appreciable at all the considered frequencies, though it is more significant at X-band [Santi et al., 2009]. Again, the higher dynamic range of the SMOS data can be observed.

The plots in Figures 6 show a higher sensitivity at H polarization and an increasing sensitivity with wavelength which is partly due to the lower SMOS observation angle. However, the higher sensitivity is also accompanied by a higher data dispersion. At Horizontal polarization, it is due to the higher sensitivity to other soil parameters, such as soil roughness which may change simultaneously with moisture content, and such variations yield stronger effects at lower frequencies and during the leaf-off period. It must be also considered that, while vegetation effects can be considered constant over few days or weeks time frame, the figures report measurements collected during two years so that, for a given SMC, differences in vegetation cover may arise which correspond to different radiometric responses, especially at lower frequencies.

Table 1 - Pearson correlation coefficient of emissivity eh vs. SMC.

	AMSR-E X Band	AMSR-E C Band	SMOS L Band
All data	0.49	0.51	0.70
Spring-Summer data	0.32	0.38	0.71
Autumn-Winter data	0.54	0.55	0.70

The Pearson correlation coefficients calculated for the above measurements at H polarization are summarized in Table 1. They confirm a certain degree of correlation between the radiometric quantity and the soil moisture, especially at the lower frequencies. Similar values are derived for PI (Tab. 2).

Table 2 - Pearson correlation coefficient of PI vs. SMC.

	AMSR-E X Band	AMSR-E C Band	SMOS L Band
All data	0.45	0.51	0.59
Spring-Summer data	0.42	0.49	0.61
Autumn-Winter data	0.44	0.50	0.55

This parameter effectively normalizes out the surface temperature, without requiring its knowledge. Results reported in Figure 3 and Table 2 show that as frequency increases PI correlation with SMC decreases. However it is still influenced by soil moisture even at C and X-band. This is because at large incidence angles (like the AMSR-E ones) there is a large difference between the vertically and horizontally polarized brightness temperatures for bare soils, providing a large PI signal notwithstanding the greater attenuation of the emission from the underlying soil.
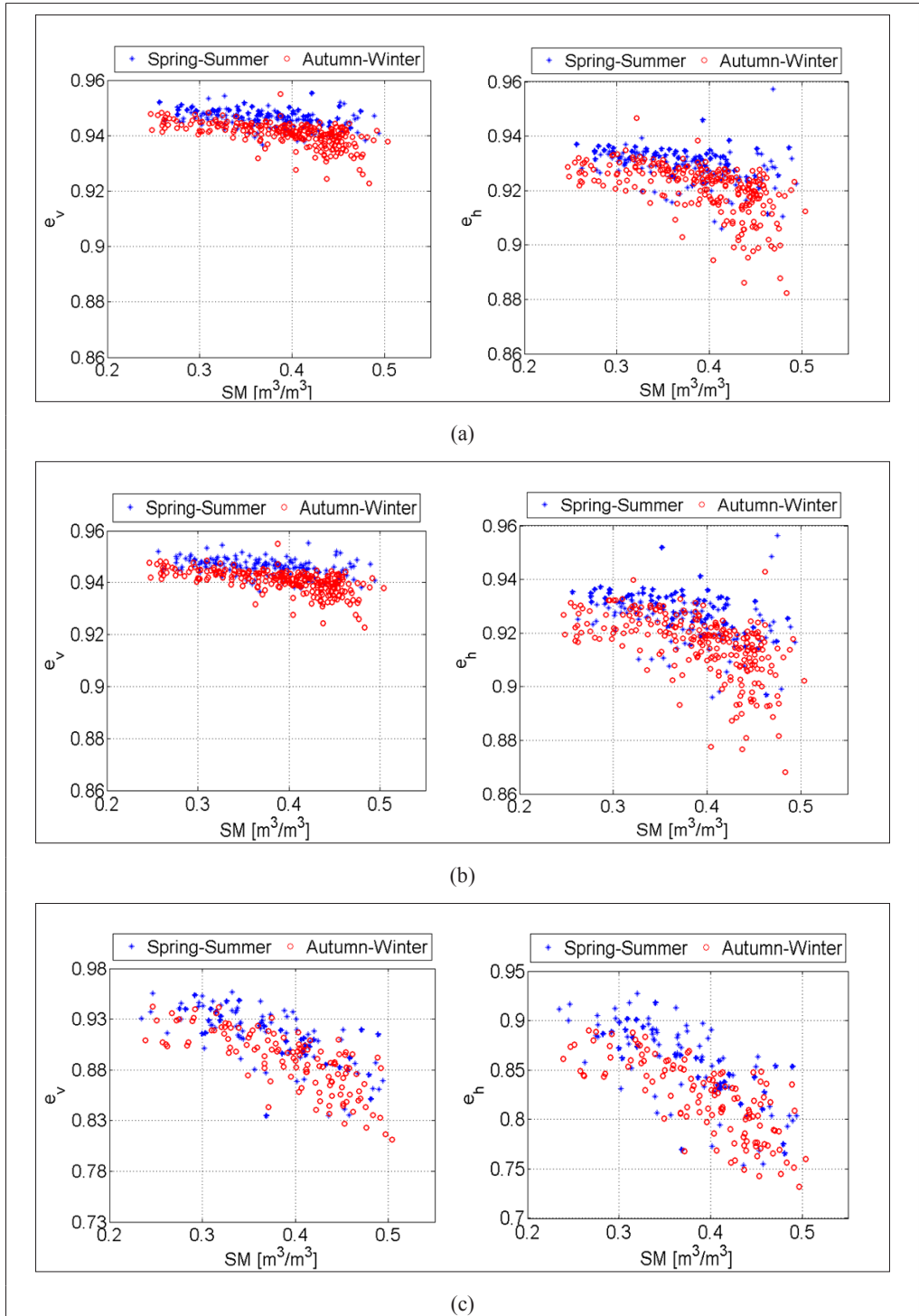
Figure 6 - a) AMSR-E X band vs. ECMWF SMC. Left: ev. Right: eh; b) AMSR-E C band vs. ECMWF SMC. Left: ev. Right: eh; c) SMOS L-band vs. ECMWF SMC. Left: ev. Right: eh.

Maps of ECMWF SMC (Fig. 7) and emissivity (Fig. 8 and 9) are displayed in the following in order to analyze the spatial variability at X and L bands (the C-band emissivity image is very similar to the X one). Two dates have been considered: the image of May 26th, 2010 (DoY = 146) was collected immediately following some rain events, thus representing a situation of high soil moisture. The second image was taken on June 15th 2010 (DoY = 166), after twenty days during which no rain occurred.
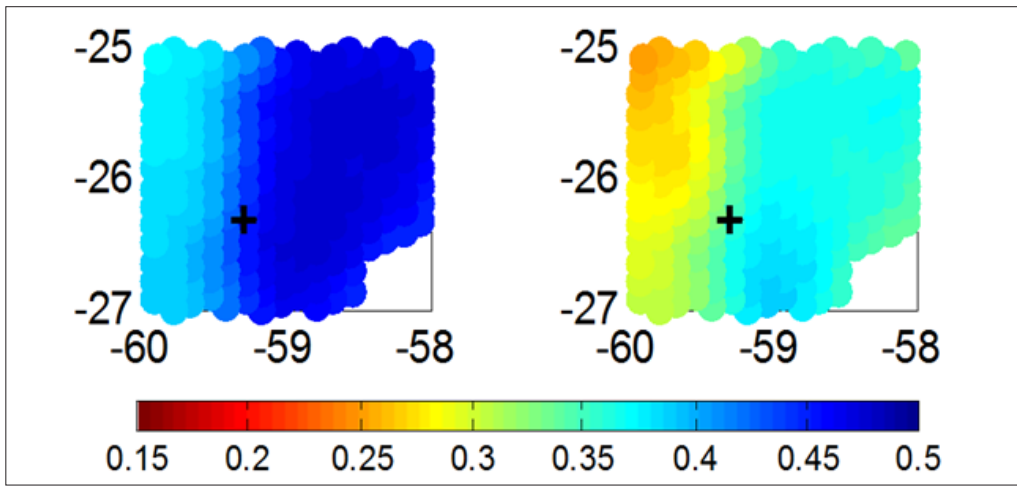

Figure 7 - ECMWF SMC maps. Left: May 26th, 2010 (after a rain event on DoY = 146). Right: June 15th 2010 (after a drying period).

The black cross in the maps refers to El-Colorado site location. During the week before May 26th, some rainstorms were recorded by the local rainfall stations. These events concurred to determine the high SMC values reproduced in the left map of Figure 7: the SMC ranges between about 0.37 to 0.47 m³/m³, with an increasing spatial trend from west to east, i.e., towards the Paraguay river which lies in the bottom right corner of the images. After about twenty days with no rainfall, the soil condition becomes drier with a SMC range between 0.27 - 0.37 m³/m³. Emissivity maps at H polarization at X band and L band can be compared in Figure 8 and 9, respectively. In general the left side images show lower values of emissivity with respect to the right ones. Furthermore, the overall spatial pattern is correlated with the Soil Moisture map showing lower emissivity values going from West to East. Both frequencies are suitable to detect the spatial variability of SMC due to rainfall. X-band AMSR-E image owns a better spatial resolution, while the SMOS data (note the expanded color scale with respect to X-band) seem to record more subtle spatial variation of SMC, making it possible to produce more detailed maps.

Conclusions
Two years of AMSR-E and SMOS data have been collected in the lower Bermejo basin (Argentina) with the aim of studying the degree of correlation between radiometer measurements and the soil moisture content in a moderately forested site. A multi-frequency

analysis has been carried out considering the emissivity and the polarization index at X, C and L band. ECMWF SMC has been considered to perform the study, while the ground truth from some rainfall stations located in the Bermejo territory have been used to validate the results. The electromagnetic signatures at the considered frequencies have been compared with respect to each other and to SMC and rainfall trends.
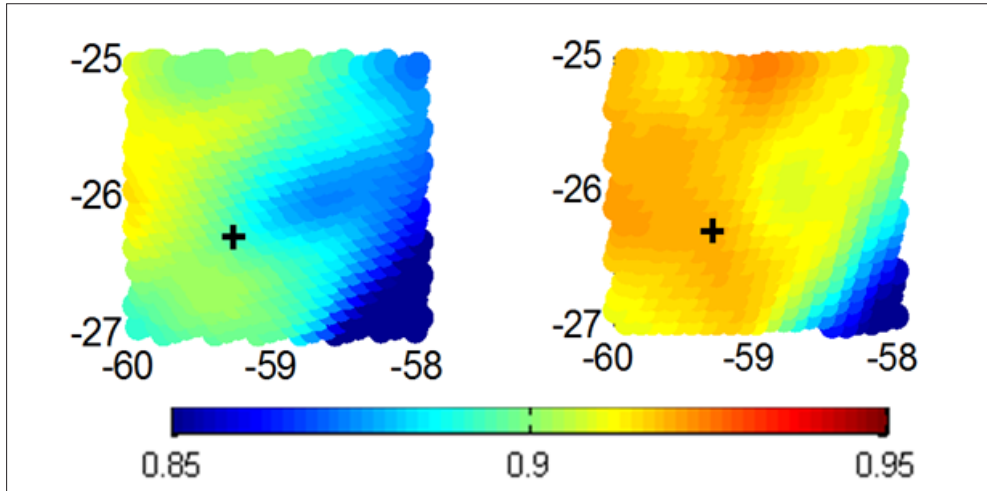

Figure 8 - X band emissivity at H polarization maps. Left: May 26th, 2010 (after a rain event on DoY = 146). Right: June 15th 2010 (after a drying period).
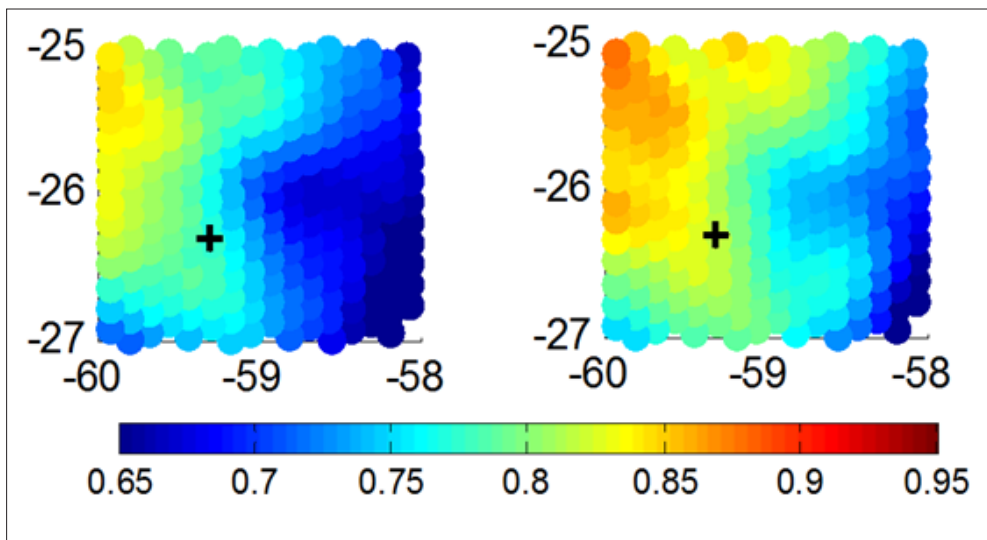

Figure 9 - L band emissivity at H polarization maps. Left: May 26th, 2010 (after a rain event on DoY = 146). Right: June 15th 2010 (after a drying period).

Although the *e* and PI values have been acquired by independent instruments, at different angles and at different times of the day, a clear temporal correlation between the AMSR-E and the SMOS data, and of both of them with the ECMWF SMC and rainfall trend has been found. As expected, the dynamic range of L band is much higher than the one attainable using X and C band. The obtained results are promising, confirming the SMOS potentiality to retrieve soil moisture under forests with moderate biomass.

References

Al Bitar A., Leroux D., Kerr Y.H, Merlin O., Richaume P., Sahoo A., Wood E.F. (2012) - *Evaluation of SMOS Soil Moisture products over continental US Using the SCAN/ SNOTEL Network*. IEEE Transaction Geoscience and Remote Sensing, 50:1572-1586. doi: http://dx.doi.org/10.1109/TGRS.2012.2191089.

Choudhury B.J. (1989) - *Monitoring global land surface using Nimbus-7 37 GHz data theory and examples*. International Journal of Remote Sensing, 10: 1579-1605. doi: http://dx.doi.org/10.1080/01431168908903993.

Della Vecchia A., Ferrazzoli P., Wigneron J.-P., Grant J.P. (2007) - *Modeling forest emissivity at L-band and a comparison with multitemporal measurements*. IEEE Geoscience and Remote Sensing Letter, 4: 508-512. doi: http://dx.doi.org/10.1109/LGRS.2007.900687.

Della Vecchia A., Ferrazzoli P., Guerriero L., Rahmoune R., Paloscia S., Pettinato S., Santi E. (2010) - *Modeling the multifrequency emission of broadleaf forests and their components*. IEEE Transaction Geoscience and Remote Sensing, 48: 260-272. doi: http://dx.doi.org/10.1109/TGRS.2009.2029343.

Ferrazzoli P., Guerriero L., Paloscia S., Pampaloni P., Solimini D. (1992) - *Modelling polarization properties of emission from soil covered with Vegetation*. IEEE Transaction Geoscience and Remote Sensing, 30: 157-165. doi: http://dx.doi.org/10.1109/36.124226.

Ferrazzoli P., Guerriero L. (1996) - *Passive microwave remote sensing of forests: A model investigation*. IEEE Transaction Geoscience and Remote Sensing, 34: 433-443. doi: http://dx.doi.org/10.1109/36.485121.

Ferrazzoli P., Guerriero L., Wigneron J.-P. (2002) - *Simulating L-band emission of forests in view of future satellite applications*. IEEE Transaction Geoscience and Remote Sensing, 40: 2700-2708. doi: http://dx.doi.org/10.1109/TGRS.2002.807577.

Grant J.P., Wigneron J.-P., Van de Griend A.A., Kruszewski A., Søbjærg S.S., Skou, N. (2007) - *A field experiment on microwave forest radiometry: L-band signal behaviour for varying conditions of surface wetness*. Remote Sensing of Environment, 109: 10-19. doi: http://dx.doi.org/10.1016/j.rse.2006.12.001.

Jackson T.J., Schmugge T.J. (1991) - *Vegetation effects on the microwave emission of soils*. Remote Sensing of Environment, 36: 203-212. doi: http://dx.doi.org/10.1016/0034-4257(91)90057-D.

Kawanishi T., Sezai T., Ito Y., Imaoka K., Takeshima T., Ishido Y., Spencer R.W. (2003) - *The Advanced Microwave Scanning Radiometer for the Earth Observing System (AMSR-E), NASDA's contribution to the EOS for global energy and water cycle studies*. IEEE Transaction Geoscience and Remote Sensing, 41: 184-194. doi: http://dx.doi.org/10.1109/TGRS.2002.808331.

Kerr Y.H., Waldteufel P., Wigneron J.P., Martinuzzi J.M., Berger M. (2001) - *Soil moisture*

retrieval from space: the soil moisture and ocean salinity (SMOS) mission. IEEE Transasction Geoscience and Remote Sensing, 39: 1729-1735. doi: http://dx.doi.org/10.1109/36.942551.

Kerr Y.H., Waldteufel P., Richaume P., Wigneron J.P., Ferrazzoli P., Mahmoodi A., Al Bitar A., Cabot F., Gruhier C., Juglea S.E., Leroux D., Mialon A., Delwart S. (2012) - *The SMOS soil moisture retrieval algorithm*. IEEE Transaction Geoscience and Remote Sensing, 50: 1384-1403. doi: http://dx.doi.org/10.1109/TGRS.2012.2184548.

Kerr Y.H., Njoku E. (1990) - *A semiempirical model for interpreting microwave emission from semiarid land surfaces as seen from space*. IEEE Transaction Geoscience and Remote Sensing, 28: 384-393. doi: http://dx.doi.org/10.1109/36.54364.

Njoku E., Jackson T.J., Lakshmi V., Chan T.K., Nghiem S.V. (2003) - *Soil moisture retrieval from AMSR-E*. IEEE Transaction Geoscience and Remote Sensing, 41: 215-229. doi: http://dx.doi.org/10.1109/TGRS.2002.808243.

Paloscia S., Pampaloni P. (1988) - *Microwave polarization index for monitoring vegetation growth*. IEEE Transaction Geoscience and Remote Sensing, 26: 617-621. doi: http://dx.doi.org/10.1109/36.7687.

Paloscia S., Pampaloni P. (1992) - *Microwave vegetation indexes for detecting biomass and water conditions of agricultural crops*. Remote Sensing of Environment, 40: 15-26. doi: http://dx.doi.org/10.1016/0034-4257(92)90123-2.

Paloscia S., Macelloni G., Santi E. (2006) - *Soil moisture estimates from AMSR-E brightness temperatures by using a dual-frequency algorithm*. IEEE Transaction Geoscience and Remote Sensing, 44: 3135-3144. doi: http://dx.doi.org/10.1109/TGRS.2006.881714.

Pampaloni P. (2004) - *Microwave radiometry of forests*. Waves Random Media, 14: S275-S298. doi. http://dx.doi.org/10.1088/0959-7174/14/2/009.

Parinussa R.M., Holmes T.R., de Jeu R.A. (2012) - *Soil moisture retrievals from the WindSat spaceborne polarimetric microwave radiometer*. IEEE Transaction Geoscience and Remote Sensing 50: 2683-2694. doi: http://dx.doi.org/10.1109/TGRS.2011.2174643.

Rahmoune R., Ferrazzoli P., Walker J.P., Grant J.P. (2010) - *L-band emission from a Eucalyptus forest in various soil conditions during the NAFE campaign*. Microwave Radiometry and Remote Sensing of the Environment (MicroRad2010) 11th Specialist Meeting, 81-85. doi: http://dx.doi.org/10.1109/MICRORAD.2010.5559584.

Santi E., Paloscia S., Pampaloni P., Pettinato S. (2009) - *Ground-based microwave investigations of forest plots in Italy*. IEEE Transaction Geoscience and Remote Sensing, 47: 3016-3025. doi: http://dx.doi.org/10.1109/TGRS.2009.2021613.